Excitation of electronic states in tetrahydrofuran by electron impact

T. P. T. Do, M. Leung, M. Fuss, G. Garcia, F. Blanco et al.

Citation: J. Chem. Phys. **134**, 144302 (2011); doi: 10.1063/1.3575454
View online: http://dx.doi.org/10.1063/1.3575454
View Table of Contents: http://jcp.aip.org/resource/1/JCPSA6/v134/i14
Published by the American Institute of Physics.

Excitation of electronic states in tetrahydrofuran by electron impact

T. P. T. Do,[1,a)] M. Leung,[1] M. Fuss,[2] G. Garcia,[2] F. Blanco,[3] K. Ratnavelu,[4] and M. J. Brunger[4,b)]

[1]*ARC Centre for Antimatter-Matter Studies, School of Chemical and Physical Sciences, Flinders University, GPO Box 2100, Adelaide, SA 5001, Australia*
[2]*Instituto de Fisica Fundamental, Consejo Superior de Investigaciones Cientificas, Madrid 28006, Spain*
[3]*Departamento de Fisica Atómica, Molecular y Nuclear, Universidad Complutense de Madrid, Madrid 28040, Spain*
[4]*Institute of Mathematical Sciences, University of Malaya, Kuala Lumpur 50603, Malaysia*

(Received 7 February 2011; accepted 21 March 2011; published online 8 April 2011)

We report on differential and integral cross section measurements for the electron impact excitation of the three lowest lying Rydberg bands of electronic states in tetrahydrofuran. The energy range of the present experiments was 15–50 eV with the angular range of the differential cross section measurements being 15°–90°. The important effects of the long-range target dipole moment and the target dipole polarizability, on the scattering dynamics of this system, are evident from the present results. To the best of our knowledge, there are no other theoretical or experimental data against which we can compare the cross section results from this study. © *2011 American Institute of Physics*. [doi:10.1063/1.3575454]

I. INTRODUCTION

Single-track simulation procedures[1–4] for photons and electrons (including secondary electrons produced through ionization), for modeling radiation damage in matter, with clear applications to the fields of radiotherapy[5–8] and radiodiagnosis, require interaction probabilities (cross sections) over a broad energy range for all accessible processes as well as the corresponding energy loss patterns.[9] These studies are particularly useful in attempting to achieve good therapeutic outcomes, where irradiated areas are reduced with the absorbed dose in surrounding healthy tissue minimized. For the particular case of DNA-damage, this requires a capacity for spatial resolutions of the order of a nanometre or better.[9] Such a level of description in turn requires a detailed knowledge of the atomic and molecular properties of the target for the simulation.

It is well known[10] that high-energy radiation produces abundant secondary electrons ($\sim 4 \times 10^4$ per MeV of energy deposited), which are the main source of the energy transfer map and radiation damage. However it is only relatively recently, thanks to the work of Sanche and colleagues,[11–13] that we began to understand that even electrons with subionization energies could produce damage, in terms of DNA strand breaks and molecular dissociation, more efficiently than the traditionally considered way of direct ionization of the medium. Unfortunately, DNA is not itself readily amenable for the sort of studies needed to determine all of the input data for the modeling work. As a consequence, moieties of DNA like tetrahydrofuran (THF), as well as water, have become the biomolecules of choice for attempting to build up the requisite data bases for track simulations in matter.[14] Of course these gas phase cross sections are an approximation to what actually might be the case in soft matter, although the recent work of White and Robson,[15] in which the collective behavior of soft matter is taken into account through "structure factors," suggests that they will have a continued utility.

Previous gas phase studies into electron scattering from THF have been quite limited, and we now summarize them briefly below. At the total cross section (TCS) level there are measurements from the work of Zecca *et al.*,[16] Fuss *et al.*,[14] and Možejko *et al.*[17] Differences between their cross sections can be understood in terms of the different angular-resolution correction effects of their apparatus, with the results from the work of Fuss *et al.* and Možejko *et al.* being closer to the true physical value because of their superior angular resolution. Absolute elastic differential cross sections (DCSs) for energies (E_0) above and equal to 20 eV were reported by Milosavljević *et al.*,[18] while Colyer *et al.*[19] reported elastic DCS data for energies between 6.5–50 eV and for scattering angles (θ) between 10°–130°. At about the same time Dampc *et al.*,[20] for $E_0 = 6 - 20$ eV and $\theta = 20° - 180°$, reported corresponding elastic measurements. Most recently, a detailed study (absolute) of both elastic excitation functions and angular distributions was reported by Allan[21] who, where a comparison could be made, found good agreement with the results of Colyer *et al.*[19] We note that some of the above groups also derived elastic integral cross section (ICS) values from their DCS measurements. Vibrational excitation function measurements have been reported by Dampc *et al.*,[22] with a comprehensive series of excitation functions, for six of the normal modes of THF, at $\theta = 135°$ and for $E_0 \cong$ threshold − 16 eV, also being given by Allan.[21] Significant resonance effects in the vibrational excitation functions were observed by Allan.

a)Present address: Physics Department, School of Education, Cantho University, Vietnam.
b)Electronic mail: Michael.Brunger@flinders.edu.au. Permanent address: ARC Centre for Antimatter-Matter Studies, School of Chemical and Physical Sciences, Flinders University, GPO Box 2100, Adelaide, SA 5001, Australia.

With respect to the electron impact excitation of the electronic states of THF, we know of only two measurements, a single energy loss measurement at $E_0 = 100$ eV and $\theta = 10^\circ$ from the work of Giuliani *et al.*,[23] and a more complete study by Bremner *et al.*[24] Some "bandlike" structure was apparent in the spectrum of Giuliani *et al.*, although it was not nearly as pronounced as that found in those same authors' photoabsorption studies.

From a theoretical perspective, several detailed electron scattering calculations on THF have been reported. Trevisan *et al.*[25] published results from an *ab initio* calculation of the elastic differential and momentum transfer cross sections using the complex Kohn variational method. A similar study was undertaken by Winstead and McKoy,[26] although in this case the cross sections were obtained from a Schwinger multichannel method. A detailed series of independent atom model (IAM)-screened additivity rule (SCAR) calculations, for grand total cross sections, integral elastic cross sections, and the sum of all the integral cross sections for inelastic processes (except rotations and vibrations), can be found in the work of Fuss *et al.*[14] Bouchiha *et al.*[27] used an R-matrix approach, with a Born correction, to calculate elastic and some inelastic (electronic-state) ICSs and the energies of a number of core-excited or Feshbach resonances. Finally, Tonzani and Greene[28] calculated some integral elastic cross sections and were able to provide additional insight into resonance effects on this channel.

In Sec. II of the paper, we present some information on the spectroscopy of THF, followed by a precis of our experimental methods and analysis details. Thereafter (Sec. IV), we provide our results and a discussion of those results before finishing with some conclusions.

II. SPECTROSCOPY OF THF (C_4H_8O)

The first hurdle to overcome, in attempting to understand the spectroscopy of THF, is to determine precisely what is the point-group symmetry of its global energy-minimum conformer and also its next nearest (in energy) conformers. The literature suggests several possibilities, with some work (Refs. 25 and 29 and references therein) suggesting that its ground-state equilibrium geometry belongs to the planar C_{2v} point group so that the oxygen and four carbon atoms lie in a single plane. However, other studies (Refs. 27, 30, and 31 and references therein) have suggested that there are in fact lower symmetries, including the twisted C_2 and envelope C_s structures, which have even lower absolute energies. In addition to these three conformers, a couple of measurements[32,33] have also reported the possibility that C_1 is the ground-state symmetry of THF. However, most work[23,30,34–37] does seem to support the notion that the nonplanar symmetrical C_2 point group symmetry is the global minimum (energy) conformer, with another local minimum conformer of the C_s symmetry. In any event, Bouchiha *et al.*[27] and Trevisan *et al.*[25] noted that the structural bond-lengths and bond angles for three of the different configurations (C_2, C_s, and C_{2v}) are very similar and so are their target properties. For example, the energy differences between their various ground-state structures are small (< 0.2 eV), while their permanent dipole moments change by only 0.02 D.

The theoretical work contained in the recent study of Giuliani *et al.*[23] took into account what are generally considered to be the three most common conformers in THF (C_{2v}, C_2, and C_s). They conducted a Boltzmann analysis at 298 K that indicated that both the C_2 and C_s forms were present with relative populations of 55.5% and 44.5%. The C_{2v} geometry, however, was found from their computations to be a saddle point with two imaginary frequencies and so is not expected to be present. It is therefore quite clear that the effusive, room temperature, THF molecular beam, which we employ in our scattering measurements (see Sec. III), will contain at least two conformational forms each with their own set of electronic-state configurations.[23] This already suggests some of the complexity involved in interpreting our measured energy-loss spectra.

One of the first studies into the excited electronic-state spectroscopy of gas-phase THF was performed by Pickett *et al.*[38] This investigation employed a vacuum ultraviolet (VUV) photoabsorption spectrometer, and reported two noticeable electronic bands with peaks at 6.378 and 6.899 eV, respectively (see also Ref. 23 and references therein). Subsequently, Hernandez[39] similarly worked on the VUV absorption spectra of THF. Those results also indicated the presence of the two bands, at around 6.377 and 6.899 eV, thereby confirming the work of Pickett *et al.* In addition, Hernandez noted the presence of a region consisting of several doublet bands beginning at 7.634 eV. This region ended with a very broad final band with a peak at around 7.978 eV. Thereafter, the spectra became increasingly complicated with a large number of closely spaced bands. Indeed, the energy differences between these groups gradually decrease as you go to even higher energies, until beyond 9.237 eV where the states significantly overlap.

In 1991, Bremner *et al.*[24] reported electron energy loss spectra (EELS) for THF that showed broad "absorption" bands. They suggested that the observed transitions may involve a nonbonding electron (n_0) from the oxygen atom occupying the highest occupied molecular orbital (HOMO). Bremner *et al.* and Tam and Brion[40] assigned the three lowest bands to being Rydberg in nature, the $^1n_0 \rightarrow 3s$, $^1n_0 \rightarrow 3p$, and $^1n_0 \rightarrow 3d$ bands, with respective vertical excitation energies of 6.6, 7.2, and 7.8 eV. Interestingly, Bremner *et al.* also suggested that these lower-lying excited states of THF may also contain valence excitations. Three other Rydberg states were also found by these authors[24,40] at 8.57 eV ($^1n_0 \rightarrow 4p$), 8.89 eV ($^1n_0 \rightarrow 5p$), and 8.1 eV [$^1n_0 - 1$ (or HOMO-1) $\rightarrow 3s$], with all these data being summarized in the work of Bouchiha *et al.*[27]

Excitation thresholds for the various electronic states were calculated by using pseudonatural orbitals from two models, by Bouchiha *et al.* (see this paper for full details). Unfortunately although the model, which employed equal abundances for the ground electronic states that result from the C_2 and C_s symmetries, gave fair agreement with experiment in some cases, in others the excitation threshold agreement between experiment and theory was quite poor. Bouchiha *et al.* suggested that using larger basis sets and more exact

configuration interaction models would correct these problems, but at the cost of having a much more computationally expensive calculation to run.

Giuliani *et al.*[23] published a detailed study of the ground and excited electronic states of both neutral THF and its cation. We note that this work employed state-of-the-art theoretical and experimental methods. In particular, their photoabsorption spectra, which may be the highest resolution spectra currently available (~0.075 nm), showed excellent agreement with their *ab initio* calculations and with some of the previously published data. In addition, they were able to resolve several controversies in regard to the spectroscopy of THF. Of particular importance to this study, they clearly observed the lowest-energy excited electronic states distributing themselves into three distinct bands, which we now discuss in more detail. Note that this result was in excellent agreement with the work of Bremner *et al.*[24]

The first band, covering the energy range of ~6.04–6.88 eV, was also found to be in very good agreement with the results from the Davidson *et al.*[41] study. This band, peaking at around 6.6 eV, appears to contain significant structure at high resolution and was assigned by Giuliani *et al.* as being primarily due to the excitation of 3*s*-type Rydberg states. The transitions giving rise to this band were assigned by them[23] for both the C_2 and C_s conformers, with the vertical excitation energy for the lowest 3*s* (C_s) transition being estimated to be at 6.353 eV. The second band, with a peak at ~7.15 eV, contains features that originate mainly from the excitation of the 3*p* Rydberg terms. This band also, at high resolution, contains numerous structures in the photoabsorption spectrum due to the excitation of the 3*p* states and their associated vibrational sublevels. Note that here the vertical excitation energy for the lowest 3*p* (C_s) transition is at around 7.154 eV. The 3*d* Rydberg terms, spanning from about 7.40–8.15 eV, contribute to both the second and third bands. For instance, a prominent feature in the measured photoabsorption spectrum at 7.483 eV, i.e., in the second band, is in fair agreement with the theoretical value (7.474 eV) for the excitation of the lowest 3*d* (C_2) state.[23] The third band also contains many structures when measured at high resolution, with sharp features observed at 7.730, 7.813, and 7.973 eV. The two most intense of these features, at 7.730 and 7.813 eV, match quite well with the predicted transition energies for the excitation of two 3*d* (C_2) states at 7.715 and 7.754 eV. For a more complete description of the states in each band, and also for their entire experimental and theoretical findings, please consult Giuliani *et al.*

We consider that the study of Giuliani *et al.*[23] currently provides the most thorough description for the electronic-state spectroscopy of THF. This work clearly illustrates why it would be folly for us, with our energy resolution (see Sec. III), to try and assign flux and ultimately cross sections to any individual excited electronic state. Rather, we follow their lead and attempt to interpret our EELS results in terms of three bands (which we call band 1, band 2, and band 3) of Rydberg excited states. The first band is composed of 3*s* Rydberg terms, while the second and third bands contain a mixture of 3*p* and 3*d* type Rydberg terms. These bands are illustrated on a series of typical energy-loss spectra, from the present investigation, in Fig. 1. Plots such as this are very important in charged-particle-track studies,[1–4] as they determine the energy deposition for the kinematical conditions specified. Using the results of Giuliani *et al.* we perform a spectral deconvolution on each of our measured energy-loss spectra, see Sec. III for those details, from which the DCSs for the band 1, band 2, and band 3 of Rydberg states are ultimately determined. Those results are presented and discussed later in Sec. IV.

III. EXPERIMENTAL METHODS AND ANALYSIS DETAILS

A high-resolution electron monochromator, described originally by Brunger and Teubner,[42] was employed to make the measurements. Here a beam of high-purity THF (Aldrich, stated purity > 99.99%), effusing from a molybdenum tube of ~0.6 mm internal diameter, is crossed with a beam of pseudomonoenergetic electrons of desired energy E_0. Elastically and inelastically scattered electrons at a particular scattering angle are energy analyzed and detected. The overall energy resolution of the monochromator for these experiments was ~50–60 meV (full width at half maximum) and, under normal operating conditions, incident electron beam currents of ~2nA were obtained in the interaction region for the energy range of these measurements. As in previous work,[42] the true zero scattering angle was determined as that about which the elastic scattering intensity was symmetric. The estimated error in this determination was $\pm 1^\circ$. The electron energy scale was calibrated against the well-known helium ^2S resonance at 19.367 eV (Ref. 43) and is estimated to be accurate to less than 50 meV.

At each incident energy in the range $E_0 = 15 - 50$ eV, energy-loss spectra, at each scattering angle in the range $\theta = 15 - 90^\circ$, were recorded over the range of $-0.5 - 11$ eV. Typical spectra (with the background having already been subtracted) are shown in Fig. 1, where the three bands of Rydberg states we wish to study are also denoted. It is interesting that these three bands become somewhat less distinct as the scattered electron angle increases, possibly suggesting that the excitation of some triplet valence states is also occurring. While this hypothesis, in the absence of theory, remains speculative, it is consistent to some extent with the work of Bremner *et al.*[24] who suggested that valence states might exist in this energy-loss region. The energy-loss spectra were obtained by ramping the analyzer in an energy-loss mode in conjunction with a multichannel scalar (TN-7200), which stored the scattered signal as a function of energy loss. The data were then transferred to a 433 MHz workstation for analysis. Each spectrum was then analyzed (deconvolved) by a computer least squares fitting technique that is similar in detail to that outlined by Nickel *et al.*,[44] although adapted to accommodate the particular spectroscopy of THF.[23,24] In particular, the Rydberg band profiles' shapes and widths, as well as the energy-loss value of the respective band maxima, were all gleaned and fixed as much as possible from the work of Giuliani *et al.*[23] In practice, the fitting procedure yielded the ratio (R) of the DCS for the Rydberg band of interest (band 1, band 2, or band 3, n' in general), $\sigma_{n'}(E_0, \theta)$, to that for the

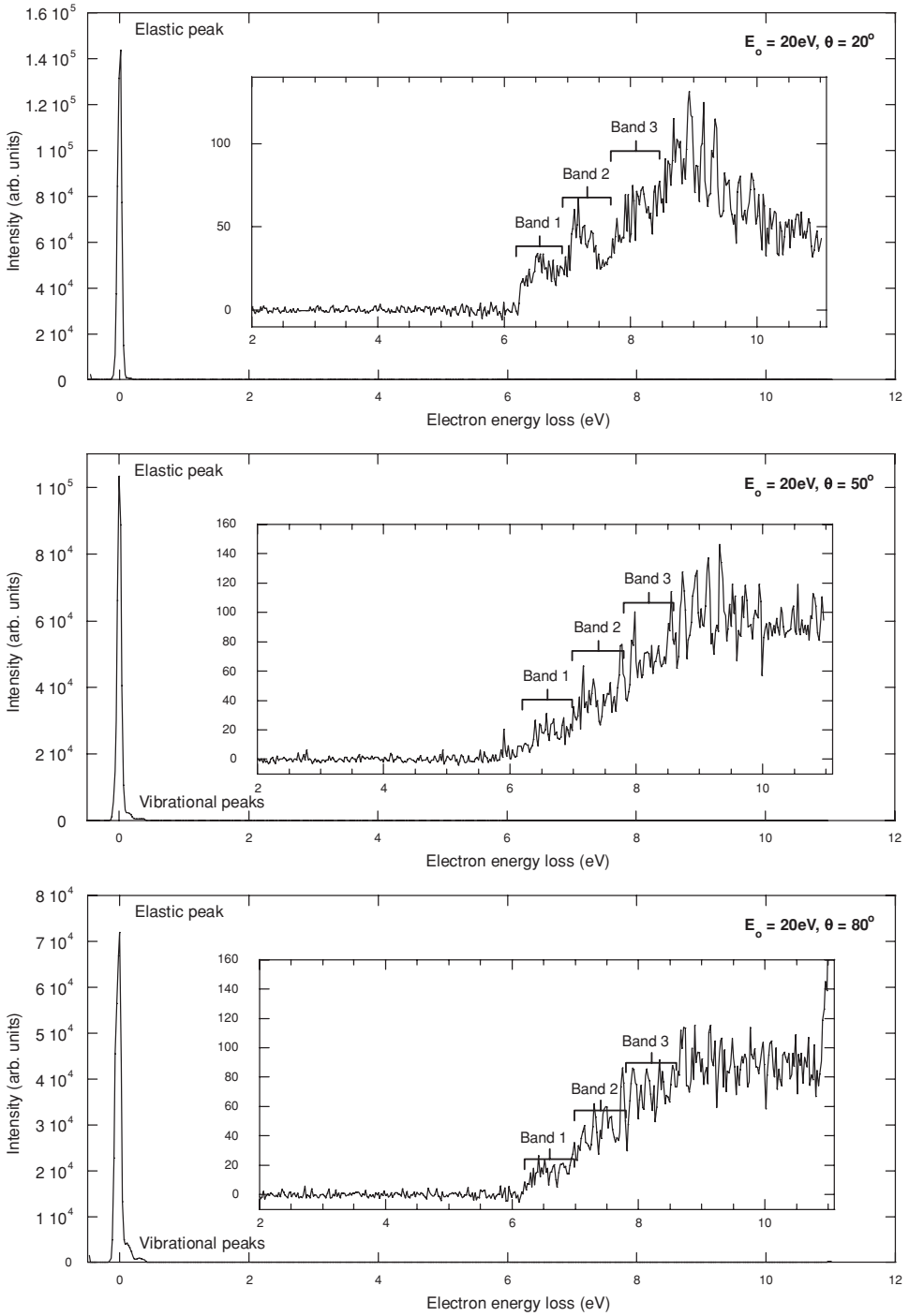

FIG. 1. Typical electron energy loss spectra for 20 eV electrons scattering from THF, obtained at a variety of kinematical conditions as denoted on the plots. The spectra are very complicated with many overlapping Rydberg terms. Different scales were employed to highlight the differences in the peak heights, of the various components in these spectra, which vary with the kinematical conditions under study. The three main bands of Rydberg terms that we study are also denoted on this figure.

elastic DCS, $\sigma_0(E_0, \theta)$. That is,

$$R_{n'}(E_0, \theta) = \frac{\sigma_{n'}(E_0, \theta)}{\sigma_0(E_0, \theta)}. \quad (1)$$

It is immediately apparent from Eq. (1) that the product $R_{n'}(E_0, \theta) \times \sigma_0(E_0, \theta)$ then gives the required Rydberg electronic band DCS provided $\sigma_0(E_0, \theta)$ is known. In the present study our preferred elastic THF differential cross sections are those obtained by Colyer *et al.*[19] Equation (1) is only valid if the transmission efficiency of the analyzer remains constant over the energy loss and the angular range studied, or is at least well characterized. In this work we determine the behavior of the analyzer response function following the philosophy outlined by Allan.[45]

Particular attention to the identification and quantification of all possible sources of error has been made throughout these measurements, with a general discussion of these sources of error being found in the work of Brunger and

Buckman.[46] In this case the statistical errors associated with the scattering intensity measurements are small ($\leq 2\%$). Additional errors due to the uncertainty in the elastic cross section by Colyer *et al.* ($\sim$6.7–11.7%) and our analyzer transmission calibration ($\sim$20%) must also be considered. Another important error in our study is that associated with the numerical deconvolution of the energy-loss spectra, with the overall errors on our DCS typically ranging from 25%–37%, depending on the E_0 and θ under consideration.

Finally, the measured DCSs are extrapolated to 0° and 180°, using a molecular phase shift analysis (MPSA) technique,[47] before performing the usual integration in order to determine the ICSs at each E_0 and for each Rydberg band. Because of the uncertainty in performing this extrapolation, particularly between the backward angles 90°–180°, the overall errors on our ICSs are typically in the range of 30–50%. Note, as we shall see shortly, all our Rydberg band DCSs are strongly peaked at the more forward scattering angles. Thus, in spite of the $\sin\theta$ weighting factor in calculating the ICSs, most of the contribution to the integrand comes from where we have measured data. If this was not the case, then the uncertainties on our ICSs would be even larger than what we cite.

IV. RESULTS AND DISCUSSIONS

In Tables I–III, we list the present differential cross sections for electron impact excitation of the Rydberg bands of states in THF. Also included in these tables are our estimates of the errors on those DCSs, with all uncertainties being cited at the one standard deviation level. As noted earlier, it was largely the comprehensive photoabsorption and quantum chemistry study by Giuliani *et al.*[23] that allowed us to identify that these bands were due to the excitation of Rydberg states, with band 1 being largely due to the excitation of 3*s* terms, band 2 being largely due to the excitation of 3*p* terms, and band 3 being largely due to the excitation of 3*d* terms. A selection of the present DCS data, for all three bands, is also given in Figs. 2 (20 eV) and 3 (50 eV).

As it should be immediately clear from Figs. 2 and 3, there are no other experimental data or theoretical computations against which we can compare the present results. Indeed, we hope that the current study will stimulate theoreticians to attempt to calculate cross sections for this scattering system, although we appreciate the difficulties they would face. As a first step, however, it might be possible for Bouchiha *et al.*[27] to extend their present 8-state and 15-state calculations to higher (>10 eV) energies. There are several other general trends in our DCSs which we can glean from Tables I–III and Figs. 2 and 3. First, at each energy studied, the DCSs for all three bands become more forward peaked in magnitude as you go to smaller scattered electron angles, with

TABLE I. Differential cross sections ($\times 10^{-19}$ cm^2/sr) for electron impact excitation of the band 1 Rydberg states in THF. Numbers in parentheses are the percentage errors on the data. Corresponding integral cross sections ($\times 10^{-18}$ cm^2) are given at the foot of the table, with the numbers in parentheses again representing the percentage uncertainties on those ICSs.

	DCS ($\times 10^{-19}$ cm^2/sr)			
	E_0 (eV)			
θ°	15	20	30	50
15	...	43.90 (28.5%)	44.80 (28.5%)	26.41 (23.2%)
20	4.85 (32.8%)	25.23 (22.4%)	20.67 (24.7%)	8.93 (24.8%)
30	3.93 (27.6%)	11.48 (27.8%)	5.18 (21.7%)	1.44 (27.4%)
40	1.94 (30.0%)	3.23 (21.6%)	2.24 (22.5%)	0.86 (24.4%)
50	2.27 (24.6%)	1.81 (39.1%)	1.83 (29.0%)	1.00 (25.7%)
60	1.39 (25.7%)	1.26 (22.5%)	1.02 (23.7%)	0.67 (27.5%)
70	1.24 (21.7%)	1.62 (22.3%)	1.08 (21.8%)	0.53 (22.6%)
80	1.24 (23.5%)	0.98 (24.0%)	0.77 (22.4%)	0.47 (21.5%)
90	1.41 (22.8%)	1.58 (23.2%)	0.98 (24.6%)	0.45 (26.6%)
ICS (10^{-18} cm^2)	4.98 (50.0%)	8.21 (44.1%)	8.00 (44.7%)	6.79 (42.7%)

TABLE II. Differential cross sections ($\times 10^{-19}$ cm^2/sr) for electron impact excitation of the band 2 Rydberg states in THF. Numbers in parentheses are the percentage errors on the data. Corresponding integral cross sections ($\times 10^{-18}$ cm^2) are given at the foot of the table, with the numbers in parentheses again representing the percentage uncertainties on those ICSs.

	DCS ($\times 10^{-19}$ cm^2/sr)			
	E_0 (eV)			
θ°	15	20	30	50
15	...	91.46 (29.2%)	116.26 (28.4%)	72.71 (22.3%)
20	8.65 (29.9%)	58.17 (22.4%)	50.73 (23.5%)	26.02 (23.8%)
30	6.08 (30.1%)	17.12 (33.7%)	11.06 (23.7%)	4.33 (24.9%)
40	2.76 (29.7%)	6.06 (21.5%)	5.50 (21.7%)	2.50 (21.6%)
50	3.96 (22.0%)	3.98 (36.9%)	3.74 (28.8%)	2.08 (23.4%)
60	3.15 (22.5%)	3.50 (22.1%)	3.25 (25.2%)	1.67 (22.2%)
70	2.79 (21.9%)	3.77 (22.4%)	2.70 (22.2%)	1.64 (22.6%)
80	2.79 (22.8%)	3.61 (25.3%)	3.03 (23.6%)	1.47 (22.0%)
90	3.16 (25.8%)	3.88 (22.9%)	2.44 (23.7%)	1.79 (21.7%)
ICS (10^{-18} cm^2)	5.32 (50.0)	19.09 (44.5%)	22.10 (45.1%)	18.03 (47.5%)

TABLE III. Differential cross sections ($\times 10^{-19}$ cm^2/sr) for electron impact excitation of the band 3 Rydberg states in THF. Numbers in parentheses are the percentage errors on the data. Corresponding integral cross sections ($\times 10^{-18}$ cm^2) are given at the foot of the table, with the numbers in parentheses again representing the percentage uncertainties on those ICSs.

	DCS ($\times 10^{-19}$ cm^2/sr)			
	E_0 (eV)			
θ°	15	20	30	50
15	...	102.54 (30.8%)	121.77 (30.0%)	96.40 (23.8%)
20	10.82 (29.8%)	81.34 (22.6%)	57.00 (23.3%)	37.29 (23.1%)
30	8.35 (30.0%)	18.60 (35.5%)	14.23 (27.3%)	6.63 (24.7%)
40	3.92 (32.9%)	7.72 (21.7%)	6.23 (21.5%)	3.68 (22.1%)
50	7.14 (21.9%)	6.50 (34.9%)	5.12 (27.9%)	3.20 (21.9%)
60	5.79 (21.5%)	4.80 (22.1%)	4.55 (29.3%)	2.76 (21.7%)
70	5.53 (21.6%)	5.18 (22.3%)	3.78 (22.3%)	2.52 (22.9%)
80	5.37 (22.0%)	4.97 (23.7%)	4.40 (24.5%)	2.46 (21.4%)
90	6.85 (25.9%)	5.79 (22.9%)	3.78 (23.1%)	2.76 (21.7%)
ICS (10^{-18} cm^2)	9.69 (50.0%)	23.26 (47.6%)	25.53 (48.8%)	23.67 (45.3%)

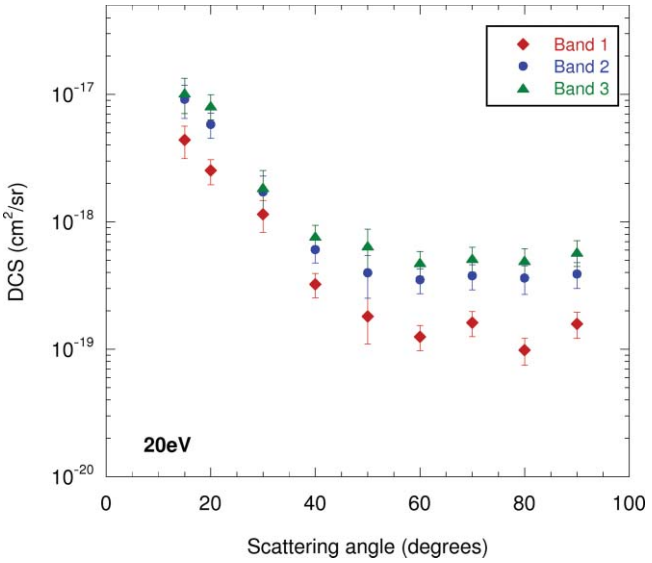

FIG. 2. Present differential cross sections (cm^2/sr) for 20 eV electron impact excitation of the three lowest-lying 3*s*, 3*p*, and 3*d* Rydberg bands of electronic states in THF. See also legend on figure for more details.

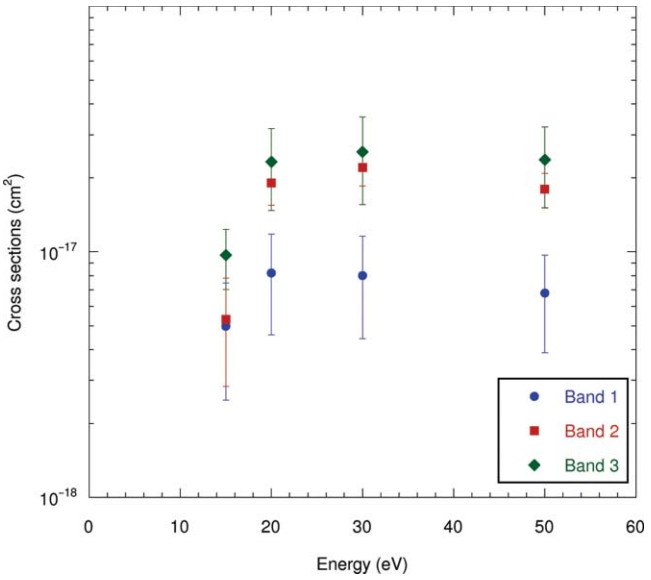

FIG. 4. Present integral cross sections (cm^2) for electron impact excitation of the three lowest-lying 3*s*, 3*p*, and 3*d* Rydberg bands of electronic states in THF. See also legend on figure for more details.

this degree of forward peaking increasing markedly as the incident electron energy increases from 15 to 50 eV. This behavior is consistent with the significant dipole moment [1.63 D (Ref. 48)] and relatively large dipole polarizability [47.080 a.u. (Ref. 49)] that the conformers of THF possess, suggesting that both these large-range interactions are important in the scattering dynamics of this system. Second, again this is a general trend at each energy, the magnitude of the DCSs, at a given scattered electron angle, are greater in band 3 than those in band 2 which are in turn greater than those in band 1. Rydberg states are often quite diffuse and so perhaps this latter observation is indicative for the 3*d*-series being relatively more diffuse than the 3*p*-series which also in turn is relatively more diffuse than the 3*s*-series. Finally, with the possible exception of the 15 eV angular distribution, none of the measured DCSs exhibit much, if any, angular structure (see Figs. 2 and 3) irrespective of the incident electron energy. Hence, there is no evidence for any resonance decay into any of these bands at the energies we studied.

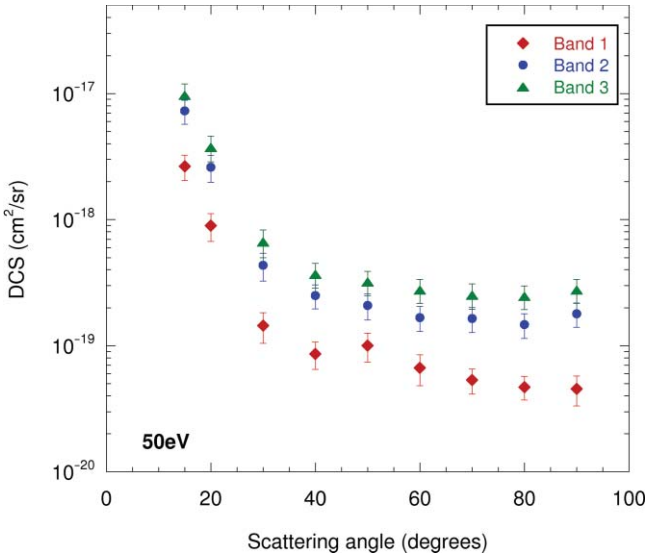

FIG. 3. Present differential cross sections (cm^2/sr) for 50 eV electron impact excitation of the three lowest-lying 3*s*, 3*p*, and 3*d* Rydberg bands of electronic states in THF. See also legend on figure for more details.

At the foot of each of Tables I–III we also list our ICS estimates, as determined using our MPSA approach,[47] for electron impact excitation of the three bands of Rydberg electronic states in THF. Corresponding errors, again at the one standard deviation level, are also provided. We note that all that data is plotted in Fig. 4.

Considering Fig. 4 in more detail, we again see that even at the ICS level there are no data against which we can compare the present results. It is also clear from this figure that each of the ICSs for bands 1, 2, and 3 are structureless, and from 20–50 eV almost uniform in magnitude. Consistent with what we found at the DCS level, the magnitude of our ICSs is largest for band 3, second largest for band 2, and smallest for band 1. No evidence for any resonances is found here (Fig. 4), although that is not too surprising given the rather coarse energy grid on which we have made our measurements.

In Fig. 5 we now plot the sum of the present electronic-state ICSs, at each energy, against earlier TCS measurements by Zecca *et al.*[16] and Fuss *et al.*,[14] an elastic ICS by Colyer *et al.*,[19] an ionization cross section measurement by Fuss *et al.*,[14] and IAM-SCAR results from those same authors[14] for the TCS, elastic ICS, and the sum of all the integral inelastic cross sections (i.e., electronic-state, ionization, and neutral dissociation). This plot suggests that the IAM-SCAR results for the TCS and elastic ICS are largely consistent with the available measured data, making them good candidates for application in any charged-particle track simulation study in THF. The IAM-SCAR result for the sum over all the inelastic cross sections is less clear cut, largely due to an absence of the experimental data to compare against. Certainly the present electronic-state ICS sum is much lower in

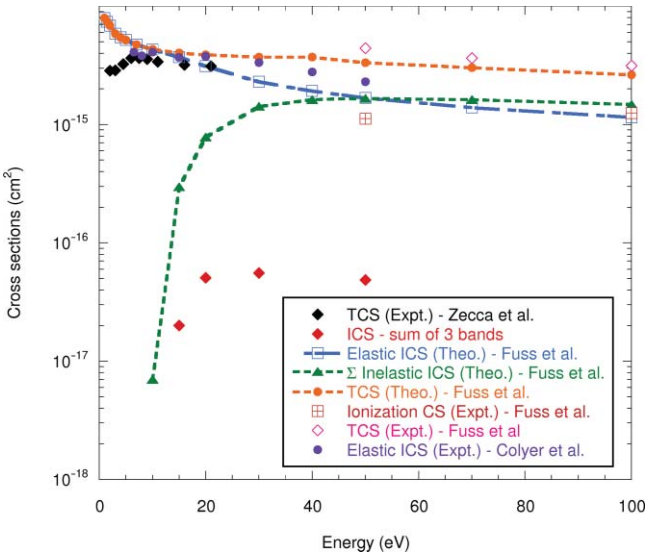

FIG. 5. Cross sections for various electron scattering processes with THF. Measured TCS data by Zecca *et al.* (Ref. 16) (black - ♦) and Fuss *et al.* (Ref. 14) (◇), elastic ICS by Colyer *et al.* (Ref. 19) (●), ionization cross sections (Ref. 14) (⊞), and the present ICSs for the sum of the three bands of electronic states (red - ♦). Also plotted are the IAM-SCAR results (Ref. 14) for the TCS (- -● - -), elastic ICS (-□—), and the sum over all the inelastic processes ICSs (▲).

magnitude compared to those theory results, and is therefore not inconsistent with the theory, which might be anticipated between 15–50 eV where ionization is probably the dominant inelastic process. Indeed at 50 eV, where the contribution from vibrational excitation and neutral dissociation might be expected to be small,[21] the sum of the ionization cross section measurements[14] with the present electronic-state ICSs is in good accord with the sum over all the inelastic ICS theory results. This gives us some confidence for a cross section database for track simulations in THF being achievable, once more comprehensive experimental data, particularly for ionization at energies ≤ 50 eV, becomes available. Note that in addition, part of the data needed for the simulation studies includes comprehensive energy loss measurements, which while we have not presented them in detail here do now exist for the energies we have studied.

V. CONCLUSIONS

We have reported on our extensive series of energy loss and differential and integral cross section measurements, in the latter cases for excitation of the three lowest lying Rydberg bands of electronic states, for electron scattering from THF. To the best of our knowledge, these cross section data are original, we could find no other calculations or experimental data to compare them against. We, in particular, hope that this study will stimulate theorists to tackle this problem, as results from such theoretical calculations will be a key in any charged-particle track simulations in THF. Certainly the present study expands the availability of the data needed to conduct such simulations. Finally, we believe that the present results showed the importance of the long-range dipole interactions on the scattering dynamics of this system.

ACKNOWLEDGMENTS

This work was conducted with support from the Australian Research Council, through its Centres of Excellence Program. Additional support from the Ministerio de Ciencia e Innovacion (Project No. FISI2009-10245) and the European Science Foundation (COST Action CM0601) is acknowledged. We are also grateful for support from a University of Malaya Research Grant (RG089/10AFR). One of us (M.J.B.) also thanks the University of Malaya for his Distinguished Visiting Professor Appointment. We all thank Dr. L. Campbell for his assistance in producing this paper.

[1] A. Muñoz, A. Williart, J. M. Pérez, F. Blanco, and G. García, J. Appl. Phys. **95**, 5865 (2004).
[2] A. Muñoz, J. M. Pérez, G. García, and F. Blanco, Nucl. Instrum. Methods Phys. Res. A **536**, 176 (2005).
[3] A. Muñoz, F. Blanco, J. C. Oller, J. M. Pérez, and G. García, Adv. Quantum Chem. **52**, 21 (2007).
[4] A. Muñoz, F. Blanco, G. García, P. A. Thorn, M. J. Brunger, J. P. Sullivan, and S. J. Buckman, Int. J. Mass Spectrom. **277**, 175 (2008).
[5] M. Georgopoulos, M. Zehetmayer, I. Ruhswurm, S. Toma-Bstaendig, N. Ségur-Eltz, S. Sacu, and R. Menapace, Ophthalmologica **217**, 315 (2003).
[6] D. B. Fuller, J. A. Kozial, and A. C. Feng, Brachytherapy **3**, 10 (2004).
[7] D. N. Slatkin, P. Spamme, F. A. Oilmanian, and M. Sandborg, Med. Phys. **19**, 1395 (1992).
[8] A. Gemmel, B. Hasch, M. Ellerbrock, W. K. Weyrather, and M. Krämer, Phys. Med. Biol. **53**, 6991 (2008).
[9] M. Fuss, A. Muñoz, J. C. Oller, F. Blanco, P. Limão-Vieira, C. Huerga, M. Téllez, M. J. Hubin-Fraskin, K. Nixon, M. Brunger, and G. García, J. Phys.: Conf. Ser. **194**, 012028 (2009).
[10] I. Plante and F. A. Cucinotto, New J. Phys. **11**, 063047 (2009).
[11] B. Boudaiffa, P. Cloutier, D. Hunting, M. A. Huels, and L. Sanche, Science **287**, 1658 (2000).
[12] B. Boudaiffa, P. Cloutier, D. Hunting, M. A. Huels, and L. Sanche, Radiat. Res. **157**, 227 (2002).
[13] M. A. Huels, B. Boudaiffa, P. Cloutier, D. Hunting, and L. Sanche, J. Am. Chem. Soc. **125**, 4467 (2003).
[14] M. Fuss, A. Muñoz, J. C. Oller, F. Blanco, D. Almeida, P. Limão-Vieira, T. P. T. Do, M. J. Brunger, and G. García, Phys. Rev. A **80**, 052709 (2009).
[15] R. D. White and R. E. Robson, Phys. Rev. Lett. **102**, 230602 (2009).
[16] A. Zecca, C. Perazzolli, and M. J. Brunger, J. Phys. B **38**, 2079 (2005).
[17] P. Możejko, E. Ptasińska-Denga, A. Domaracka, and C. Szmytkowski, Phys. Rev. A **74**, 012708 (2006).
[18] A. R. Milosavljević, A. Giuliani, D. Sević, M.-J. Hubin-Franskin, and B. P. Marinković, Eur. Phys. J. D **35**, 411 (2005).
[19] C. J. Colyer, V. Vizcaino, J. P. Sullivan, M. J. Brunger, and S. J. Buckman, New J. Phys. **9**, 41 (2007).
[20] M. Dampc, A. R. Milosavljević, I. Linert, B. P. Marinković, and M. Zubek, Phys. Rev. A **75**, 042710 (2007).
[21] M. Allan, J. Phys. B **40**, 3531 (2007).
[22] M. Dampc, I. Linert, A. R. Milosavljević, and M. Zubek, Chem. Phys. Lett. **443**, 17 (2007).
[23] A. Giuliani, P. Limão-Vieira, D. Duflot, A. R. Milosavljević, B. P. Marinković, S. V. Hoffmann, N. Mason, J. Delwiche, and M.-J. Hubin-Franskin, Eur. Phys. J. D **51**, 97 (2009).
[24] L. J. Bremner, M. G. Curtis, and I. C. Walker, J. Chem. Soc., Faraday Trans. **87**, 1049 (1991).
[25] C. S. Trevisan, A. E. Orel, and T. N. Rescigno, J. Phys. B **39**, L255 (2006).
[26] C. Winstead and V. McKoy, J. Chem. Phys. **125**, 074302 (2006).
[27] D. Bouchiha, J. D. Gorfinkiel, L. G. Caron, and L. Sanche, J. Phys. B **39**, 975 (2006).
[28] S. Tonzani and C. H. Greene, J. Chem. Phys. **125**, 094504 (2006).
[29] M. Lepage, S. Letarte, M. Michaud, F. Motte-Tollet, M.-J. Hubin-Franskin, D. Roy, and L. Sanche, J. Chem. Phys. **109**, 5980 (1998).
[30] B. Cadioli, E. Gallinella, C. Coulombeau, H. Jobic, and G. Berthier, J. Phys. Chem. **97**, 7844 (1993).
[31] E. Gallinella, B. Cadioli, J. P. Flament, and G. Berthier, J. Mol. Struct.: THEOCHEM **315**, 137 (1994).
[32] G. G. Engerholm, A. C. Luntz, W. D. Gwinn, and D. O. Harris, J. Chem. Phys. **50**, 2446 (1969).

[33]R. Meyer, J. C. Lopez, J. L. Alonso, S. Melandri, P. G. Favero, and W. Caminati, J. Chem. Phys. **111**, 2446 (1999).
[34]A. H. Mamleev, L. N. Gunderova, and R. V. Galley, J. Struct. Chem. **42**, 365 (2001).
[35]D. G. Melnik, S. Gopalakrishnan, T. A. Miller, and F. C. De Lucia, J. Chem. Phys. **118**, 3589 (2003).
[36]S. J. Han and Y. K. Kong, J. Mol. Struct.: THEOCHEM **369**, 157 (1996).
[37]A. Wu and D. Cremer, Int. J. Mol. Sci. **4**, 158 (2003).
[38]L. W. Pickett, N. J. Hoeflich, and T. C. Liu, J. Am. Chem. Soc. **73**, 4865 (1951).
[39]G. J. Hernandez, J. Chem. Phys. **38**, 2233 (1963).
[40]W.-C. Tam and C. E. Brion, J. Electron Spectrosc. Relat. Phenom. **3**, 263 (1974).
[41]R. Davidson, J. Høg, P. A. Warsop, and J. A. B. Whiteside, J. Chem. Soc., Faraday Trans. 2 **68**, 1652 (1972).
[42]M. J. Brunger and P. J. O. Teubner, Phys. Rev. A **41**, 1413 (1990).
[43]J. N. H. Brunt, G. C. King, and F. H. Read, J. Phys. B **10**, 1289 (1977).
[44]J. C. Nickel, P. W. Zetner, G. Shen, and S. Trajmar, J. Phys. E **22**, 730 (1989).
[45]M. Allan, J. Phys. B **38**, 3655 (2005).
[46]M. J. Brunger and S. J. Buckman, The Nucleus **34**, 201 (1997).
[47]L. Campbell, M. J. Brunger, A. M. Nolan, L. J. Kelly, A. B. Wedding, J. Harrison, P. J. O. Teubner, D. C. Cartwright, and B. McLaughlin, J. Phys. B **34**, 1185 (2001).
[48]J. Richardi, P. H. Fries, and H. Krienke, J. Phys. Chem. B **102**, 5196 (1998).
[49]A. Zecca, L. Chiari, A. Sarkar, and M. J. Brunger, J. Phys. B **41**, 085201 (2008).